Optical coherent transient continuously programmed continuous processor

K. D. Merkel and W. R. Babbitt

Department of Physics, Montana State University, Bozeman, Montana 59717-3840

Received September 25, 1998

A novel technique for continuously programming an optical coherent transient spatial–spectral signal processor is proposed. The repeated application of two spatially distinct optical programming pulses to a nonpersistent hole-burning material writes an accumulated spatial–spectral population grating. An optical data stream is introduced on a third beam, resulting in a processor output signal that is spatially distinct from all the input pulses. Programming and processing take place simultaneously, asynchronously, and continuously. In the case of true-time delays, the efficiency that is achievable with currently available materials is of the order of that predicted for a perfect photon-gated device. © 1999 Optical Society of America

OCIS codes: 030.0030, 090.0090, 070.6020, 050.2770.

Optical coherent transient (OCT) devices such as a memory,[1] a signal cross correlator,[2–4] and an optical true-time delay regenerator[5,6] have been proposed and demonstrated. Although each device has different aspects in its programming and processing stages, all are implementations of a generalized OCT processor. A continuous OCT processor has been proposed[3] and demonstrated.[4] In that system two spatially distinct programming beams are used to write a spatial–spectral population grating, and so the emitted output signal is spatially distinct from the subsequently applied continuous input data stream, and thus they can temporaly overlap. Such a system offers one the ability to process fully a temporarily structured waveform (TSW) that is modulated in amplitude and phase at projected data rates greater than 10 GHz and with time–bandwidth products greater than 10,000.[3]

OCT devices can process data only as long as the programmed spatial–spectral grating survives. When the programming stage is a single-shot event, writing a strong grating in a nonpersistent hole-burning material, the processing stage can occur until the excited absorbers decay to their ground states. After the grating decays away fully, the programming stage can be repeated, but this leads to dead time for the processor that is several times the excited-state lifetime, T_1. An alternative implementation is to utilize persistent spectral holes. But for single-photon persistent holes (e.g., hyperfine storage), the processing stage is partially destructive to the stored grating.[4] For two-photon persistent holes (i.e., gated storage),[7] the processing stage is nondestructive and can be continuous,[3] but low writing and gating efficiencies of available materials make this impractical currently. Each of the above techniques requires strong programming pulses, a disadvantage that could be lessened if the grating were accumulated by repetition of the programming and gating processes. However, the temporal distinction between the programming and the processing stages remains for all the above techniques, along with the constraints on efficiency, materials, and devices.

In this Letter we propose a method for achieving continuous processing in non-persistent hole burning materials with an inhomogeneously broadened transition (IBT). The stored grating is accumulated and refreshed by repeated application of the programming sequence.[8] The input beam geometry isolates the emitted signal from all the input waveforms so that the optical signal processor can simultaneously, asynchronously, and continuously process an input signal while it is being continuously programmed.

In general, an OCT processor is programmed with two temporally modulated optical pulses that are separated in time and resonant with an IBT. Each laser pulse has a form $E_n(t - t_n - \eta_n)\cos[\omega_0(t - \eta_n) + \phi_n]$, where the subscript n determines the order of arrival of each pulse, $E_n(\tau)$ is a slowly varying temporal envelope function, ω_0 is the laser center frequency, $\eta_n = (\hat{k}_n \cdot \mathbf{r}/c)$, where $\hat{k}_n$ is the unit wave vector of pulse n, ϕ_n is the phase of pulse n, and each pulse reaches the medium at $\mathbf{r} = 0$ at its arrival time t_n. The two waveform envelopes, $E_1(\tau)$ and $E_2(\tau)$, separated by $\tau_{21} = t_2 - t_1$, write a spatial–spectral holographic population grating on the IBT. A programming pulse can be a temporally brief reference pulse (BRP), a linear frequency-chirped reference pulse, or a TSW that represents data.

After a grating is programmed, the atomic absorption is selective in both frequency and space for subsequently applied optical waveforms. As long as the grating survives, a subsequently applied $E_3(\tau)$ causes a coherent emission $E_s(t - t_s - \eta_s)\cos[\omega_0(t - \eta_s) + \phi_s]$ from the IBT with the temporal envelope of the form

$$E_s(t - t_s - \eta_s) \propto \int_{-\infty}^{\infty} E_1{}^*(\Omega)E_2(\Omega)E_3(\Omega) \times \exp[i\Omega(t - t_s - \eta_s)]\,\mathrm{d}\Omega\,, \qquad (1)$$

where $t_s = t_3 + t_2 - t_1$, $\eta_s = \eta_3 + \eta_2 - \eta_1$, $\phi_s = \phi_3 + \phi_2 - \phi_1$, and $E_n(\Omega)$ is the Fourier transform of the nth applied optical waveform envelope, $E_n(\tau)$. Relation (1) is based on the Fourier transform approximation of the input waveforms,[1,2] valid when these bandwidths less than the inhomogeneous linewidth, $\delta\omega_I$, and intensities that ensure a linear response, avoiding both coherent and incoherent saturation.[3]

0146-9592/99/030172-03$15.00/0

The phase-matching condition for the proposed continuous processing and programming technique is $\hat{k}_s = \hat{k}_3 + \hat{k}_2 - \hat{k}_1$, where all three input pulses are distinct such that $\hat{k}_1 \neq \hat{k}_2 \neq \hat{k}_3$. Figure 1(a) shows a three-dimensional representation of this scheme. Perfect phase matching is achieved if the pulses are directed such that for a given vector $\mathbf{k}_0$, the individual wave vectors are $\hat{k}_n = \mathbf{k}_0 + \delta\mathbf{k}_n$, where for $n = 1, 2, 3$, every $|\delta\mathbf{k}_n|$ is equal, $\delta\mathbf{k}_n \perp \mathbf{k}_0$, and $\delta\mathbf{k}_3 = -\delta\mathbf{k}_2$. In addition, we achieve phase-matched angular multiplexing by varying $\delta\mathbf{k}_1$ while maintaining the above conditions.

The complete spatial–temporal implementation of the input pulses is shown in Fig. 1(b), for the specific case of signal cross correlator. In this schematic a pair of programming pulses $E_1^{(j)}(\tau)$ and $E_2^{(j)}(\tau)$ is repeated at regular intervals τ_R. In this case, the first (second) programming pulse is a TSW (BRP) on beam 1 (beam 2). Once the grating is accumulated, the waveform to be processed can be propagated along beam 3. Here the programmed pattern is included twice in this waveform. Figure 1(c) shows the shape and timing of the resulting output signal emitted along $\hat{k}_s$ with respect to the third pulse after it exits the medium. Here this signal consists of two autocorrelation peaks and other correlation signals, provided that the accumulated grating is saturated.

One must satisfy certain conditions to obtain efficient processing. First, consider the programming timing limitations with respect to material parameters. We define a generalized three-level system in which the radiation field couples only states $|1\rangle$ and $|2\rangle$ and there is an intermediate state $|3\rangle$, with population relaxation times ${\kappa_{21}}^{-1}$, ${\kappa_{23}}^{-1}$, and ${\kappa_{31}}^{-1}$ between the numbered states. This system reduces to a two-level system if $\kappa_{23} = 0$. The upper- and intermediate-state lifetimes are $T_1 = (\kappa_{21} + \kappa_{23})^{-1}$ and $T_B = {\kappa_{31}}^{-1}$. In general, the quantity $(\tau_{21} + \delta\tau_1 + \delta\tau_2)$ is limited by the homogeneous dephasing time, T_2. The inclusion of pulse duration $\delta\tau_n$ of pulses 1 and 2 accounts for the general case in which $\delta\tau_n \ll \tau_{21}$ is not satisfied. Requiring that $T_2 \geq 40(\tau_{21} + \delta\tau_1 + \delta\tau_2)$ makes the loss of efficiency that is due to coherent decay less than 10%, although techniques exist to compensate for this loss.[9] Setting $\tau_R \geq 2T_2$ avoids coherent interference between successive pairs of programming pulses. Setting τ_R much less than T_G, the greater of T_1 or T_B ensures that the repeated programming pulse pairs at the appropriate intensity form an accumulated grating,[8] where after reaching steady state, their application exactly compensates for the relaxation losses during τ_R. The relaxation losses during τ_R cause a fractional drop in the intensity of the output signal, ε. For ε to be small, τ_R must be chosen appropriately.

Beyond the population decay dynamics, the stability of the optical source is an important consideration, analogous to the discussion in Ref. 10. In practice, each repeated programming sequence may not be identical. The stored grating from a single pair of programming pulses, $G(\Omega) \propto {E_1}^*(\Omega)E_2(\Omega) \times \exp[i(\Omega\tau_{21} + \phi_{21})] + \text{c.c.}$, depends on the phase difference $\phi_{21} = \phi_2 - \phi_1$ between the two pulses. This phase difference can fluctuate owing to short-term frequency drift of the optical carrier. If the carrier frequency changes to $(\omega_0 + \delta\omega_0)$, a change in the phase difference between the programming pulses of $\delta\phi_{21} = \delta\omega_0 \cdot \tau_{21}$ will result. Consider any two programming pulse pairs, labeled the jth and the kth pairs, that occur within a time shorter than T_G. If $\phi_{21}^{(k)}$ differs from $\phi_{21}^{(j)}$ by roughly π, then the pulse pairs' contribution leads to incoherent accumulation of the grating and ineffective processing. The requirement exists, therefore, that $[\phi_{21}^{(k)} - \phi_{21}^{(j)}] \ll \pi$, implying that the short-term laser frequency stability should follow $\delta\omega_0 \ll \pi/(\tau_{21} + \delta\tau_1 + \delta\tau_2)$ over any time period T_G. When a single optical source creates the programming and processing beams, its long-term frequency drift is inconsequential, provided that all pulse bandwidths stay well within $\delta\omega_I$. As the laser drifts, the previous grating decays and the new grating seamlessly accumulates when the above condition is maintained.

Assuming a stable optical source, a continuously programmed continuous processor has the ability to produce a highly efficient grating. For continuously programmed memories and processors, when pulse 1 or 2 is a TSW, optimizing the efficiency must be balanced with nonlinearities that lead to signal distortion. But for the case of a true-time delay device when the first two pulses are both BRP's,

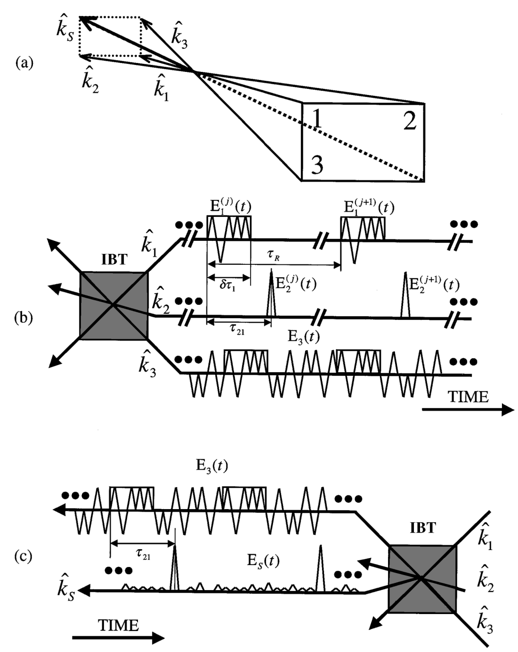

Fig. 1. (a) Perfect phase-matching geometry for three distinct input beams and the direction of emitted output signal $\hat{k}_s$. (b) Schematic and parameters of a continuously programmed continuous processor, as a signal cross correlator. Pairs of programming pulses are repeated along beams 1 and 2 to accumulate a grating. In any pair, pulse 1, on beam 1, is a pattern waveform that interferes with pulse 2, on beam 2, a brief reference pulse. Once the grating is accumulated, a continuous waveform to be processed is introduced along beam 3. (c) Schematic of the emitted output signal that is due to the inputs in (b) in relation to the waveform on beam 3 after the IBT. Outputs along beams 1 and 2 are not shown.

the efficiency analysis follows from the treatment of accumulated gratings described in Ref. 8, in which the steady-state population solutions were derived for a three-level system. For an absorber at frequency ω, the steady-state spectral population difference between the excited and the ground states is

$$\omega(\Delta) = (1 - p)\,\frac{\exp(-x_1)[1 - \exp(-x_B)] + \beta[\exp(-x_B) - \exp(-x_1)]/2}{1 - \exp(-x_B) - p\exp(-x_1)[1 - \exp(-x_B)] + \beta(1 - p)[\exp(-x_B) - \exp(-x_1)]/2} - 1, \quad (2)$$

where $\Delta = \omega - \omega_0$, $\beta = \kappa_{23}/(\kappa_{23} + \kappa_{21} - \kappa_{31})$, $x_B = \tau_R/T_B$, $x_1 = \tau_R/T_1$, and $p = 1 - 2\theta^2 \cos^2(\Delta\tau_{21}/2 + \phi_{21})$, assuming that $\theta_1 = \theta_2 = \theta$, where θ_n is the area of pulse n, $\theta \le 0.1\pi$ and $\tau_{21} \ll T_2$. Equation (2) reduces to the two-level case when $\beta = 0$.

A qualitative estimate of the intensity of the true-time delay output signal is the magnitude squared of the inverse Fourier transform of Eq. (2), evaluated at τ_{21}. For reference, the efficiency is normalized against that of a photon-gated two-level persistent hole-burning system with gating efficiency $\gamma_{\text{gate}} = 1$.[3] In general, given fixed values for T_1, T_B, and β, we can optimize the efficiency to η_{opt} for any given τ_R by varying θ to a value θ_{opt}. Increasing τ_R increases both θ_{opt} and ε. It is found that η_{opt} is identical for all τ_R and $\eta_{\text{opt}} = 0.47$. Thus, nonpersistent materials can have efficiencies higher than that of a photon-gated material with $\gamma_{\text{gate}} < 0.68$, since the output intensities of gated systems go as γ_{gate}^2. Currently available gated materials have $\gamma_{\text{gate}} \ll 1$,[7] so in comparison with these the efficiency of a continuously programmed grating is several orders of magnitude greater. For $T_B >> T_1$, the efficiency is due almost entirely to the first harmonic of the accumulated grating in the ground state, not the upper state. For $\beta = 0$ or for $T_B \ll T_1$, both ground- and upper-state population gratings contribute to the efficiency.

Consider two nonpersistent material system that are currently available at wavelengths compatible with commercially available diode lasers. For a three-level system, Tm^{3+}:YAG (0.1 at.%) offers an intermediate bottleneck level between the two levels of the IBT at 793 nm. At 4.4 K, $\delta\omega_I \sim 17$ GHz, $T_2 \sim 16$ μs, $T_1 \sim 800$ μs, $T_B \sim 9$ ms, and $\beta \sim 0.59$.[11,12] Setting $\tau_R = 32$ μs yields $\theta_{\text{opt}} = 0.05\pi$ and $\varepsilon = 2.0\%$. Delays of up to 0.4 μs are feasible without any compensation,[9] provided that the laser frequency is stable to 250 kHz over 9 ms. For a two-level system, Er^{3+}:$LiNbO_3$ (0.06 at.%) has an IBT at 1.53 μm. At 1.6 K, $\delta\omega_I \sim 200$ GHz, $T_1 \sim 10$ ms ($\beta = 0$), and $T_2 \sim 40$ μs in a 3-kG external magnetic field.[13] Setting $\tau_R = 80$ μs yields $\theta_{\text{opt}} = 0.045\pi$ and $\varepsilon = 1.6\%$. Delays of over 1.0 μs[9] are feasible for a laser that is stable to 100 kHz for 10 ms. For both cases the efficiencies are still better than that of a gated material with $\gamma_{\text{gate}} < 0.68$.

This analysis and the predicted efficiencies are valid for the OCT true-time delay regenerator[5] programmed with BRP's as well as with frequency-chirped reference pulses.[6] The input beam geometry has the benefit that nonlinearities introduced by the multiple programming stages do not lead to harmonics of the delay in the output signal direction in the case of true-time delay regenerators.

In summary, we have proposed a novel OCT technique for programming and processing. Utilizing distinct processing and programming beams makes it possible to simultaneously program a grating while asynchronously processing a continuous waveform against it. New delays or patterns can be reprogrammed into the material in a time roughly equal to the greater of T_B or T_1. This technique alleviates the need for photon gating in several types of OCT devices, specifically optical dynamic random-access memory, waveform cross correlators, and true-time delay regenerators. Multigigahertz, efficient, real-time processing with large-bandwidth products (>10,000) can be achieved in currently available nonpersistent materials.

We gratefully acknowledge the support of this work by the Air Force Office of Scientific Research, the University of Colorado–Boulder, and the U.S. Office of Naval Research under the Multidisciplinary University Research Initiative program.

References

1. T. W. Mossberg, Opt. Lett. **7,** 77 (1982).
2. Y. S. Bai, W. R. Babbitt, N. W. Carlson, and T. W. Mossberg, Appl. Phys. Lett. **45,** 714 (1984).
3. W. R. Babbitt and J. A. Bell, Appl. Opt. **33,** 1538 (1994).
4. M. Zhu, W. R. Babbitt, and C. M. Jefferson, Opt. Lett. **20,** 2514 (1995).
5. K. D. Merkel and W. R. Babbitt, Opt. Lett. **21,** 1102 (1996).
6. K. D. Merkel and W. R. Babbitt, Opt. Lett. **23,** 528 (1998).
7. W. E. Moerner, ed., *Persistent Spectral Hole-burning: Science and Applications*, Vol. 44 of Topics in Current Physics (Springer-Verlag, Berlin, 1988), and references therein.
8. W. H. Hesselink and D. A. Wiersma, J. Chem. Phys. **75,** 4192 (1981).
9. K. D. Merkel and W. R. Babbitt, Opt. Commun. **128,** 136 (1996).
10. U. Elman, B. Luo, and S. Kroll, J. Opt. Soc. Am. B **9,** 1905 (1996).
11. J. A. Caird, L. G. Deshazer, and J. Nella, IEEE J. Quantum Electron. **QE-11,** 874 (1975).
12. R. M. Macfarlane, Opt. Lett. **18,** 1958 (1993).
13. Y. Sun, Montana State University, Bozeman, Mont. 59717 (personal communication, November 10, 1998).